Nov 5th, 12:00 AM - 12:00 AM

On the Influence of Local-Distortional Interaction in the Behavior and Design of Cold-Formed Steel Web-Stiffened Lipped Channel Columns

André D. Martins

Pedro Borges Dinis

Dinar Camotim

Paulo Providência

On the Influence of Local-Distortional Interaction in the Behavior and Design of Cold-Formed Steel Web-Stiffened Lipped Channel Columns

André D. Martins[1], Pedro Borges Dinis[1], Dinar Camotim[1] and Paulo Providência[2]

Abstract

This paper reports the results of a numerical (ABAQUS shell finite element analysis) investigation on the influence of local-distortional (L-D) interaction in the ultimate strength and design of cold-formed steel fixed-ended web-stiffened lipped channel columns – hereafter termed "WSLC columns". These results concern columns with various geometries and yield stresses, ensuring a wide variety of combined ratios between (i) the distortional and local critical buckling stresses, and (ii) the yield and the higher of the above buckling stresses. The objectives of this work are two-fold: (i) to acquire in-depth understanding on the mechanics underlying the L-D interaction in the WSLC columns analyzed, all selected to ensure that local buckling is triggered by the flanges, and also (ii) to provide a first contribution towards the efficient Direct Strength Method (DSM) design of these structural elements. The results presented and discussed concern the (i) post-buckling behavior (elastic and elastic-plastic), (ii) ultimate strength and (iii) failure mechanisms of the WSLC columns previously selected to undergo L-D interaction. Special attention is paid to comparing the ultimate strength erosions, due to L-D interaction, exhibited by the WSLC columns investigated here and the "plain cross-section" (*i.e.*, without intermediate stiffeners) columns studied earlier by the authors (Martins *et al.* 2014a). Finally, the paper closes with some considerations about the impact of the findings reported in this work on the design of cold-formed steel columns undergoing different levels of L-D interaction.

Introduction

Cold-formed steel structural systems commonly used in the construction industry are very often formed by slender open-section thin-walled members, which exhibit a low torsion stiffness and a high susceptibility to instability phenomena involving cross-section deformation, namely local, distortional and/or global buckling – Figs. 1(b)-(d) show

[1] DECivil, ICIST, Instituto Superior Técnico, Universidade de Lisboa, Av. Rovisco Pais, 1049-001 Lisboa, Portugal.
[2] Department of Civil Engineering, FCT, University of Coimbra, Rua Luís Reis Santos, 3030-788 Coimbra, Portugal.

171

buckled web-stiffened lipped channel (WSLC) cross-sections associated with column local (flange-triggered), distortional and global (flexural-torsional and flexural) modes. Moreover, cold-formed steel member often display geometries (cross-section shape and/or dimensions, and unrestrained length) that lead to fairly close local (L) and distortional (D) critical buckling stresses, which means that their post-buckling behavior (elastic or elastic-plastic), ultimate strength and failure mode are likely to be affected, to a smaller or larger extent, by interaction effects involving these two instability phenomena, *i.e.*, by local-distortional (L-D) interaction.

A considerable amount of research activity has been recently devoted to the structural response and load-carrying capacity of cold-formed steel columns affected by L-D interaction, including experimental investigations, numerical simulations and design proposals. However, the vast majority of the available results concerns columns with plain lipped channel columns – for instance, the works reported by Kwon & Hancock (1992), Yang & Hancock (2004), Dinis *et al.* (2007), Yap & Hancock (2009, 2011), Kwon *et al.* (2009), Silvestre *et al.* (2012), Young *et al.* (2013) and Martins *et al.* (2014a). Although to a lesser extent, research work has also been reported on columns with other cross-sections shapes: (i) Dinis *et al.* (2011) (hat-sections), (ii) Dinis *et al.* (2014a) (rack-sections), and (iii) Dinis *et al.* (2012) and Dinis & Camotim (2014) (zed, hat and rack-sections). For all the above cross-section shapes, local buckling is practically always triggered by the web, where most of the L-D interaction takes place. This situation may change when intermediate stiffeners (*e.g.*, "v-shaped" stiffeners) are added (see Fig. 1(a)), since local buckling is bound to be triggered by the flanges, with very little deformation occurring in the web (see Fig. 1(b)), which naturally alters considerably the L-D interaction features – this fact has been demonstrated both experimentally and numerically by Kwon & Hancock (1992), Kwon *et al.* (2009), Yap & Hancock (2011) and Dinis *et al.* (2014b).

Since the assessment of the structural response and strength of cold-formed steel members constitutes a complex task, which is not yet adequately reflected in several current design codes, a fair amount of research has been devoted to develop efficient (safe and economic) design rules for such members. The most relevant fruit of this research activity was the DSM, which (i) has its roots in the work of Hancock *et al.* (1994), (ii) was originally proposed by Schafer & Peköz (1998), and (iii) has already
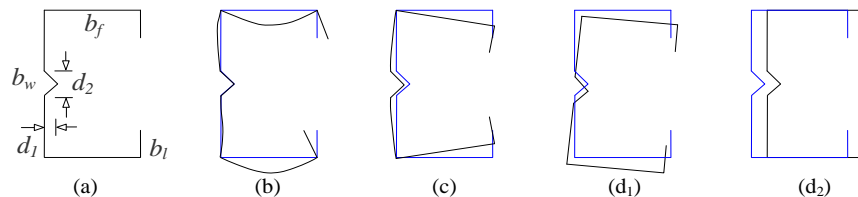

Fig. 1. Web-Stiffened lipped channel (a) geometry and buckled shapes associated with column, (b) local (flange-triggered), (c) distortional and (d) global (d$_1$) flexural-torsional and (d$_2$) flexural buckling

been included in the latest versions of the Australian/New Zealand and North American cold-formed steel specifications. The DSM has been shown to provide an efficient and general approach to estimate the ultimate strength of cold-formed steel columns and beams failing in local (L), distortional (D), global (G) and local-global (L-G) interactive modes. Unfortunately, the consideration of these limit states is not sufficient for the design of such members, since interaction phenomena involving distortional buckling, namely, L-D, D-G and L-D-G interactions may also erode significantly the member ultimate strength − neglecting these interaction phenomena may lead to unacceptably low reliability indices, *i.e.*, to a high likelihood of reaching unsafe designs.

This work deals solely with the design of columns against L-D interactive failures. Although several attempts have been made to develop a DSM-based design approach that covers also column L-D interactive failures, it is consensual that further research is still needed before the DSM can be successfully and generally applied to members affected by this type of mode interaction. In the particular case of lipped channels columns (either pin-ended or fixed-ended) experiencing L-D interaction, the second and third authors performed extensive numerical simulations that (i) made it possible to obtain clear evidence that the current DSM local and distortional design curves cannot capture the ultimate strength erosion due to this coupling behavior and (ii) unveiled features that must appear in a DSM design approach intended for such members. These findings were incorporated into a DSM-based design approach recently proposed by Silvestre *et al*. (2012), termed here "MNDL approach", only for plain lipped channel columns (exhibiting web-triggered local buckling). The above approach was later extended to plain zed, hat and rack-section columns by Dinis & Camotim (2014) − it is worth noting that these proposals concern exclusively columns affected by L-D interaction stemming from fairly close local and distortional critical buckling stresses, *i.e.*, columns affected by "true" L-D interaction (Martins *et al.* 2014a). Recently, Martins *et al.* (2014a) extended the scope of the previous findings and assessed the performance of the MNDL design approach for plain lipped channel, hat, zed and rack-section columns affected by L-D interaction caused by a "secondary bifurcation", which (i) occurs when the local and distortional critical buckling stresses are not so close and (ii) stems from the high (moderate) local (distortional) post-critical strength reserve, provided that the yield stress is sufficiently high to allow that it comes into play. It was found that the above approach provides good estimates for a fairly wide range of ratios between the local and distortional critical buckling stresses and constitutes, at present, the most efficient (safe and accurate) DSM-based design approach against L-D interactive failures. However, this approach was developed, calibrated and validated solely on the basis of analyses involving plain cross-section columns − the main purposes of this work is to assess whether this approach can be readily extended to WSLC columns.

The objectives of this paper are (i) to present and discuss numerical results aimed at acquiring in-depth understanding on the mechanics underlying L-D interaction in web-stiffened lipped channel columns (flange-triggered local buckling) and (ii) to provide a

first contribution towards the efficient DSM design of such structural elements[3]. A systematic numerical investigation is carried out, in order to characterize the post-buckling behavior and strength of WSLC columns experiencing more or less severe L-D interaction effects. Moreover, it is also intended to assess whether the available findings and design procedures, developed and proposed in the context of "plain cross-section" columns, can be readily extended to the columns under consideration. The results presented and discussed, obtained through ABAQUS shell finite element analyses, concern the (i) post-buckling behavior (elastic and elastic-plastic), (ii) ultimate strength and (iii) failure mechanisms of WSLC columns selected to undergo considerable L-D interaction. Special attention is devoted to comparing the ultimate strength erosions, due to L-D interaction, in plain and WSLC columns − the former were recently investigated by Martins *et al.* (2014a). This comparison is essential to assess whether the DSM-based design approaches developed for L-D interactive failures of "plain cross-section" columns are also applicable to their WSLC counterparts. Finally, the paper closes with some considerations concerning the impact of the findings reported in this work on the possibility of developing a general DSM-based design approach capable of efficiently (safely and accurately) predicting the load-carrying capacity of "plain cross-section" and WSLC cold-formed steel columns undergoing various levels of L-D interaction.

Buckling Analysis – Column Geometry Selection

In order to investigate the numerical ultimate strength of fixed-ended WSLC columns affected by various levels of L-D interaction, the first step consists of selecting column geometries (cross-section dimensions and length) associated with different "levels of closeness" between their local and distortional critical buckling stresses (*i.e.*, $R_{DL}=f_{crd}/f_{crl}$ values). As done in previous studies, the column geometry selection was made by means of a "trial-and-error" procedure involving the performance of GBT-based buckling analysis sequences using the code GBTUL (Bebiano *et al*. 2008), which makes it possible to determine buckling loads associated with "pure" local, distortional and global buckling modes. Fig. 2(a) shows the GBT discretization adopted for all WSLC columns analyzed, which (i) comprises 21 (9 natural and 12 intermediate) nodes, and (ii) leads to 21 deformation modes (4 global, 5 distortional and 12 local) − Fig. 3 shows the in-plane deformed shapes of all these modes. The "pure" f_{crl}, f_{crd} and f_{crg} are obtained through GBT analyses including the following deformation modes:

(i) f_{crg}: modes **2**+**4**, for the WSLC columns, since the critical global mode is flexural-torsional (of course, very long columns buckle in minor-axis flexural modes).

(ii) f_{crd}: unlike in plain lipped channel columns (see Young *et al.* 2013), for which all distortional modes are considered to determine f_{crd}, in WSLC columns some of the

---

[3] It is worth noting that the authors (Martins *et al.* 2014b) have recently reported the first results of this investigation, concerning columns with very close local and distortional critical buckling stresses.

five distortional modes (modes **5** to **9** – see Fig. 3) are only termed "distortional" because they exhibit natural node in-plane displacements (the natural nodes are shown in Fig. 2(a)). For instance, modes **8** and **9** are clearly "disguised local modes" with web single and double curvature – note that these deformation modes are the web-stiffened counterparts of the plain modes **7** and **8**. Therefore, the determination of f_{crd} was made by means of buckling analyses including only deformation modes **5**+**6**.

(iii) f_{crl}: in view of the content of the previous item, the buckling analyses providing f_{crl} include exclusively deformations modes **7** to **21**. Due to the very short local half-wave length, the column longitudinal discretization must be finer than that adopted to calculate f_{crd} and f_{crg} – 40-60 beam finite elements were considered.

The output of this effort are the 35 distinct combinations of cross-section dimensions (b_w, b_f, b_l, t – web-flange-lip widths and wall thickness) and lengths (L) given in Table 1 – the "v-shaped" intermediate stiffeners have d_1=10mm and d_2=20mm (see Fig. 1(a)) for all columns. The half-wave numbers of the critical local (n_l) and distortional (n_d) buckling modes are also presented. These fixed-ended cold-formed steel (E=210GPa, v=0.3) columns (i) exhibit R_{DL} values such that 0.40<R_{DL}<2.40 and (ii) have global critical buckling stresses (ii$_1$) much higher than their local and distortional counterparts ($f_{crg}/f_{cr.max}$>5.2, with $f_{cr.max}$=max($f_{crl};f_{crd}$)) and (ii$_2$) higher than all the yield stresses considered ($f_{crg}/f_{y.max}$>1.1), thus ensuring that no interaction with global (flexural-torsional) modes occurs – the values of these two ratios are also given in the table. In order to enable an in-depth investigation of the influence of strong L-D interaction (0.90≤R_{DL}≤1.10), 12 columns were selected in this R_{DL} range. Fig. 2(b) shows (i) a curve providing the variation of P_{cr} (critical buckling load) with the column length L (in logarithmic scale) for a fixed-ended WSLC column with R_{DL}=1.00 (column WS16 – see Table 1), and (ii) the column "mixed" buckling mode for L_{DL}=80cm, which combines 1D
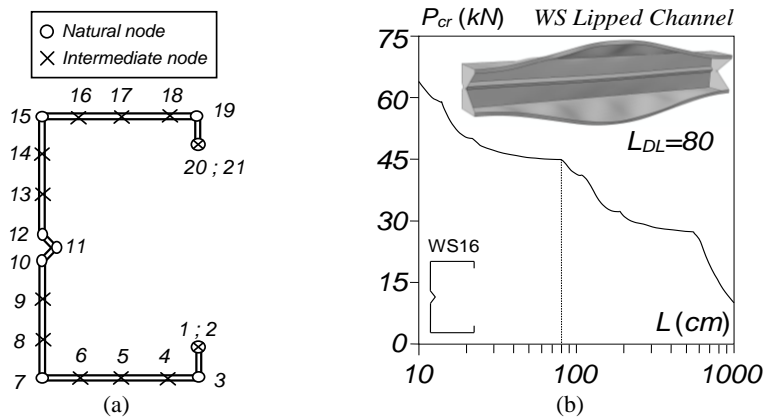

Fig. 2. WSLC column (a) GBT discretization and (b) critical buckling curve P_{cr} vs. L (WS16)
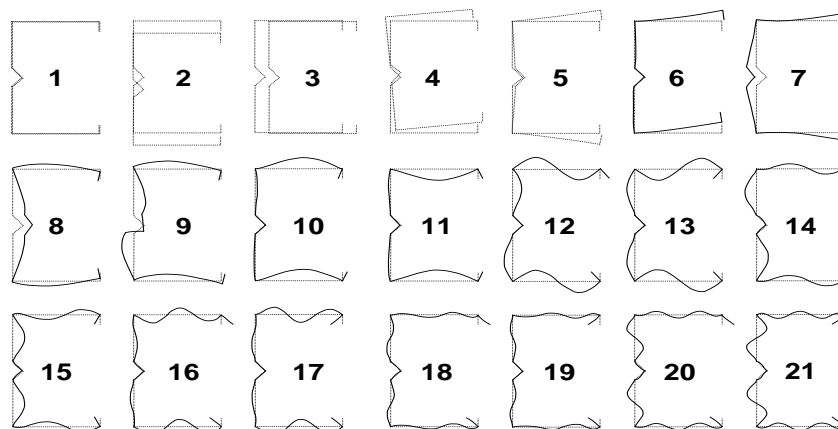
Fig. 3. In-plane deformed configurations concerning GBT conventional deformation modes

half-wave and 10 L half-waves. It seems clear that the post-buckling behavior (elastic or elastic-plastic) and ultimate strength of this columns will be strongly affected by L-D interaction, taking place predominantly in the flanges.

Post-Buckling Behavior of WSLC Columns under L-D Interaction

Finite Element Modeling

This chapter presents and discusses the main results of the numerical investigation aimed at acquiring in-depth understanding on the mechanics underlying the flange-triggered L-D interaction in fixed-ended web-stiffened lipped channels columns. The results were obtained through ABAQUS (Simulia Inc 2008) analyses using the SFE elastic-plastic model adopted earlier by Dinis *et al.* (2007) and involving (i) columns discretized into fine meshes of 4-node isoparametric shell (S4) (length-to-width ratio close to 1), (ii) end supports simulated by rigid plates attached to the end section centroids and (iii) the steel material behavior modeled by a linear-elastic/perfectly-plastic stress-strain curve (both residual stresses and corner strength effects are disregarded).

Elastic-Plastic Post-Buckling Interactive Behavior

This section addresses the elastic-plastic post-buckling behavior of the fixed-ended WSLC columns considered in this work. Fig. 4(a) shows the P/P_{cr} vs. v/t equilibrium paths (v is again the mid-span flange-lip corner vertical displacement) of WS16 columns (R_{DL}=1.00) (i) containing pure distortional initial geometrical imperfections involving inward flange-lip motions – this shape leads to the lowest columns strengths as was reported by Martins *et al.* (2014b) and (ii) exhibiting yield stresses corresponding to 9 critical slenderness values $\lambda_{cr}=(f_y/f_{cr})^{0.5}$ (recall that for these columns: $f_{cr}=f_{crd}=f_{crl}$), which cover a wide range: $1.00, 1.25, 1.50, 1.75, 2.00, 2.50, 3.00, 3.25, 3.50, \infty$ –

Table 1. WSLC columns selected column geometries, local/distortional/global buckling
stresses, buckling mode half-wave numbers and relevant stress ratios

	b_w	b_f	b_l	t	L	f_{crd}	n_d	f_{crl}	n_l	R_{DL}	f_{crg}	$\dfrac{f_{crg}}{f_{cr.max}}$	$\dfrac{f_{crg}}{f_{y.max}}$
WS1	170	130	12.0	2.400	1.70	136	2	343	11	0.40	1766	5.2	1.1
WS2	150	110	10.0	1.940	1.20	138	2	309	9	0.45	2723	8.8	1.7
WS3	150	110	10.0	2.000	1.00	165	2	329	7	0.50	3919	11.9	2.0
WS4	150	100	11.0	1.780	1.15	170	2	309	12	0.55	2914	9.4	1.5
WS5	150	100	10.0	1.510	1.15	133	2	221	12	0.60	2880	13.0	1.9
WS6	160	130	10.0	1.390	1.45	73	2	112	12	0.65	2150	19.2	2.5
WS7	160	130	10.0	1.400	1.20	80	1	113	10	0.70	3138	27.7	3.4
WS8	120	90	10.0	1.200	1.20	129	2	173	14	0.75	1816	10.5	1.2
WS9	150	95	12.0	1.360	1.10	157	1	196	12	0.80	3164	16.2	1.7
WS10	150	95	12.0	1.280	1.10	148	1	173	12	0.85	3164	18.3	1.8
WS11	120	90	10.0	1.100	0.90	128	1	142	11	0.90	3226	22.7	2.1
WS12	120	90	10.0	1.100	0.85	132	1	142	10	0.93	3616	25.5	2.2
WS13	120	90	10.0	1.100	0.80	137	1	142	10	0.96	4081	28.7	2.5
WS14	160	125	12.5	1.375	1.00	113	1	115	8	0.98	4583	40.0	3.3
WS15	120	90	10.0	1.075	0.80	134	1	136	10	0.99	4081	30.1	2.5
WS16	120	90	10.0	1.050	0.80	129	1	129	10	1.00	4081	31.7	2.6
WS17	160	125	12.5	1.325	1.00	109	1	106	8	1.02	4583	42.1	3.5
WS18	120	90	10.0	1.025	0.80	129	1	124	10	1.05	4081	31.6	2.7
WS19	160	125	12.5	1.300	1.00	108	1	103	8	1.06	4583	42.2	3.7
WS20	120	90	10.0	1.000	0.80	126	1	118	10	1.07	4081	32.3	2.8
WS21	150	95	12.0	1.030	1.10	122	1	112	12	1.09	3162	26.0	2.3
WS22	120	90	10.0	0.950	0.85	117	1	106	10	1.10	4080	34.9	3.1
WS23	120	90	10.0	0.895	0.90	115	1	96	11	1.20	3224	28.1	2.8
WS24	120	90	10.0	0.830	0.85	106	1	81	10	1.31	3614	34.0	3.6
WS25	120	90	10.0	0.800	0.90	107	1	76	11	1.40	3224	30.2	3.4
WS26	120	90	10.0	0.790	0.85	113	1	75	10	1.50	3614	32.1	4.0
WS27	150	100	10.0	0.766	0.90	89	1	56	10	1.60	4695	52.5	6.9
WS28	150	100	10.0	0.737	0.90	88	1	52	10	1.70	4695	53.4	7.4
WS29	160	125	12.3	0.950	1.00	102	1	56	9	1.82	4581	45.0	6.8
WS30	160	125	12.5	1.011	0.90	121	1	64	8	1.90	5656	46.8	7.4
WS31	160	125	12.5	1.030	0.85	132	1	66	7	2.00	6341	48.0	8.0
WS32	160	125	12.5	1.000	0.85	131	1	62	7	2.10	6341	48.4	8.4
WS33	160	120	12.5	1.000	0.85	148	1	67	7	2.20	7096	48.0	8.8
WS34	160	125	12.5	1.000	0.80	144	1	62	7	2.30	7158	49.8	9.5
WS35	160	125	12.5	0.927	0.85	128	1	53	7	2.40	6340	49.5	9.8

the last corresponds to elastic behavior. As for Fig. 4(b), it displays the deformed configurations and plastic strain distributions, at the onset of collapse, for columns with $\lambda_{cr}=1.00$, 1.75, 3.00, 3.50 – note the $\lambda_{cr}=1.00$ deformed configuration depicted in Fig. 4(b) is amplified 30 times. On the other hand, Fig. 4(c) concerns the column with $\lambda_{cr}=3.25$ and displays four plastic strain diagrams, corresponding to the equilibrium states indicated on its equilibrium path (see Fig. 4(a)), including (i) an elastic state, (ii) a state immediately after first yielding, (iii) the onset of collapse and (iv) a state on the equilibrium path descending branch. The observation of these post-buckling results prompts the following remarks:
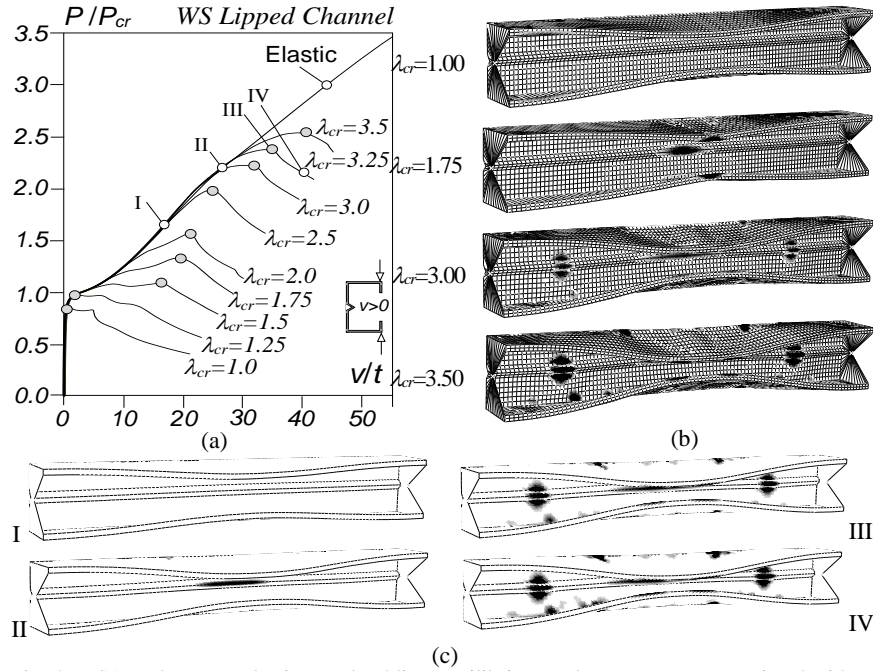
Fig. 4. WS16 column (a) elastic post-buckling equilibrium paths P/P_{cr} vs. v/t associated with D and 9 slenderness values, (b) failure modes and plastic strains for $\lambda_{cr}=\{1.0, 1.75, 3.0, 3.5\}$ and (c) deformed configurations and plastic strains evolutions at four equilibrium states ($\lambda_{cr}=3.25$)

(i) First of all, the 9 WSLC columns with distinct yield stresses are affected by L-D interaction, particularly visible in the flanges (see Fig. 4(b)). These coupling effects (i_1) are "intrinsic to the column", due to the closeness between the local and distortional critically buckling loads, (i_2) gradually evolve as loading progresses and (i_3) take place regardless of the yield stress value (provided, of course, that f_y/f_{cr} is not significantly below 1.0, in which case collapse basically involves plasticity), *i.e.*, this phenomena corresponds to "true L-D interaction" as was reported by Martins *et al.* (2014a) for "plain cross-section" columns.

(ii) The nature and characteristics of the column elastic-plastic post-buckling behavior and collapse mechanism of clearly depend on the slenderness value (λ_{cr}).

(iii) In the $\lambda_{cr}=1.00$ and $\lambda_{cr}=1.25$ columns (*i.e.*, when λ_{cr} is close to 1.0), yielding starts when the normal stress distribution is still "not too far from uniform" and, therefore, precipitates a rather abrupt (plastic) collapse (see Fig. 4(a)).

(iv) On the other hand, in the columns with higher λ_{cr} values first yielding takes place when the normal stress distribution is already "highly non-uniform" and, thus, does not lead to an immediate failure – collapse occurs following a fairly smooth stiffness decrease. Note that the WSLC columns have a significant elastic-plastic

strength reserve (see Fig. 4(a)) – *e.g.*, the λ_{cr}=3.25 column exhibits a 14% applied load difference between first yielding and the onset of collapse, which is obviously due to the fairly high D and L (mostly) post-critical strength reserves.

(v) In the λ_{cr}=3.25 column, the elastic regime (diagram I in Fig. 4(c)) ends when yielding initiates at the intermediate stiffener mid-span regions (diagram II in Fig. 4(c)). Then, plasticity spreads rapidly towards the web-flange corners over the whole column length and yielding also occurs near the end section intermediate stiffeners (diagram III in Fig. 4(c)). This behavior is clearly distinct from that exhibited by the plain lipped channels columns, which stems from the different stress distribution evolutions. Moreover, the comparison between the results presented in this paper and those reported by Silvestre *et al.* (2012), for plain lipped channel columns, makes it possible to conclude that the addition of the web intermediate stiffener leads to a reasonable post-buckling strength increase, most likely due to the higher web transverse bending stiffness, which entails much smaller effective centroid shifts (a major source of stiffness and strength erosion).

Direct Strength Method (DSM) Design

The development of the Direct Strength Method (DSM) was motivated by the need to overcome the difficulties (and time consumption) associated with the application of the classical Effective Width Method (EWM) to more complex cross-sections such as those commonly used in cold-formed steel construction, *i.e.*, exhibiting large numbers of walls, including more or less involved lips and/or intermediate stiffeners. The method has been shown to provide efficient (safe and accurate) estimates of the ultimate strength of cold-formed steel columns and beams on the sole basis of the steel yield stress and elastic critical buckling stresses (for the whole cross-section, rather than (i) the individual walls/plates and (ii) simply supported boundary conditions between walls/plates, like in the traditional EWM) associated with local, distortional and global modes.

For columns, the DSM nominal strengths against local (f_{NL}) and distortional (f_{ND}) failures are provided by "Winter-type" expressions (calibrated against a fairly large numbers of experimental and numerical failure loads, mostly involving fixed-ended columns) that can be found in Schafer's state-of-the-art report (Schafer 2008). Moreover, two distinct strategies were proposed by Schafer (2002) to estimate the ultimate strength of columns experiencing L-D interaction: replacing f_y by either (i) f_{ND} in the f_{NL} equations (NLD approach – f_{NLD}) or (ii) f_{NL} in the f_{ND} equations (NDL approach – f_{NDL}). Later, Silvestre *et al.* (2012) assessed the performance of these two approaches, for fixed-ended plain lipped channel columns, and concluded that they provide similar results, even if the quality of the f_{NDL} estimates was found to be marginally higher – quite recently, Dinis & Camotim (2014) extended these findings to hat, zed and rack-section fixed-ended columns.

A novel design approach intended specifically to handle L-D interactive failures was (i) recently developed by Silvestre *et al.* (2012), for fixed-ended plain lipped channel

columns, and (ii) subsequently extended by Dinis & Camotim (2014) to cover also hat, zed and rack-section fixed-ended columns. This approach, termed here "modified NDL approach" (MNDL), (i) coincides with f_{ND} for $\lambda_D<1.5$ and, for the more slender columns ($\lambda_D\geq1.5$), (ii) defines a modified local strength f^*_{NL}, which depends on the critical half-wave length ratio L_{crD}/L_{crL} (obtained from simply supported column signature curves) and estimates the column ultimate strength by replacing of f_{NL} with f^*_{NL} in the NDL equations. This modified local strength, which leads to f_{ND} and f_{NDL} estimates for $L_{crD}/L_{crL}\leq4$ and $L_{crD}/L_{crL}\geq8$, respectively, is given by (1)

$$f^*_{NL}=\begin{cases} f_y & , & \frac{L_{crd}}{L_{crl}}\leq 4 \\ f_y+\left(1-0.25\frac{L_{crd}}{L_{crl}}\right)\times\left(f_y-f_{NL}\right), & 4<\frac{L_{crd}}{L_{crl}}<8 \\ f_{NL} & , & \frac{L_{crd}}{L_{crl}}\geq 8 \end{cases} \quad (1) \qquad f^*_{NL}=\begin{cases} f_y & , & \frac{L_{crd}}{L_{crl}}\leq a \\ f_y+\left(\frac{a}{b-a}-\frac{1}{b-a}\frac{L_{crd}}{L_{crl}}\right)\times\left(f_y-f_{NL}\right), & a<\frac{L_{crd}}{L_{crl}}<b \\ f_{NL} & , & \frac{L_{crd}}{L_{crl}}\geq b \end{cases} \quad (2)$$

It is worth noting that the MNDL approach was developed, calibrated and validated on the basis of numerical (SFEA) ultimate strength values concerning fixed-ended "plain cross-section" columns exhibiting R_{DL} values comprised between 0.90 and 1.10. This means that the numerical results were restricted to columns strongly affected by L-D interaction, for which the ultimate strength erosion is most severe (all are included in the "true L-D interaction" region – see Martins *et al.* 2014a). Recently, the authors (Martins *et al.* 2014a) extended the previous findings and assessed the performance of the MNDL for "plain cross-section" columns affected also by a "secondary bifurcation", which occurs when the local and distortional critical buckling stresses are not so close and stems from the high (moderate) local (distortional) post-critical strength reserve. It was found that the above MNDL approach provides also good estimates far from its original domain of application, namely inside the range $0.70<R_{DL}<1.60$. As mentioned by Martins *et al.* (2014b), the application of the MNDL approach cannot be readily extended to stiffened columns, since the L_{crD}/L_{crL} limits appearing in (1) may not be suitable for web-stiffened lipped channel columns. Fortunately, it is possible to retain the elegance of the MNDL approach and still obtain efficient estimates for these stiffened cross-sections. It suffices to find new L_{crD}/L_{crL} limits that are best suited for the stiffened columns, as had already been anticipated by Silvestre *et al.* (2012) – obviously, this procedure may be viewed an optimization problem. Before finding the new L_{crD}/L_{crL} limits, where (i) "a" stands for the lower limit and (ii) "b" identifies the upper limit (see Fig. 5), it is necessary to generalize the MNDL approach to other cross-section shapes. This generalization is carried out by changing the "modified local strength" (f^*_{NL}), defined in (1), while retaining the essence of the MNDL approach: (i) $L_{crD}/L_{crL}\leq a$ leads to f_{ND} estimates and (ii) $L_{crD}/L_{crL}\geq b$ leads to f_{NDL} estimates. This generalization is expressed by in (2) – note that if $a=4$ and $b=8$ leads to (1).

The optimization problem, allowing for the determination of the design variable $\boldsymbol{x}=[a,b]$, is formulated as a minimization problem for which the objective function is
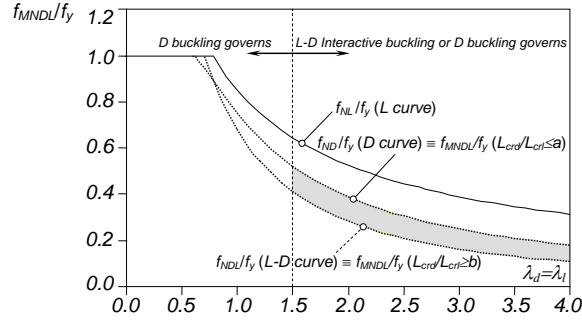
Fig. 5. Generalized MNDL approach: variation of f_{MNDL}/f_y with the column slenderness for $\lambda_d \equiv \lambda_l$ (adapted from Silvestre *et al.* (2012))

$$f(\boldsymbol{x}) = \sum_{i=1}^{n} \left(f_{U,i}^{SFEA} - f_{U,i}^{MNDL}(\boldsymbol{x}) \right)^2 \tag{3}$$

which means that the minimization problem becomes simply

$$\begin{aligned} min \; & f(\boldsymbol{x}) \\ s.a.: \quad & b - a > 0 \\ & a, b \geq 0 \end{aligned} \tag{4}$$

where (i) $f_{U,i}^{SFEA}$ and $f_{U,i}^{MNDL}$ are the *ith* numerical ultimate strength and corresponding MNDL estimate (based on the modified local strength defined in (2)) and (ii) n is the total number of numerical ultimate strengths. It is worth noting that:

(i)   Only function $f_{U,i}^{MNDL}$, discontinuous at λ_D=1.5, depends on the design variables.

(ii) The design variables are discrete (but greater than one), even if the homologous problem with continuum variables provides better MNDL estimates.

(iii) Due to the content of items (i) and (ii), the minimization problem was solved employing Genetic Algorithms (GAs) − popular stochastic search algorithms based on Darwin's evolution theory idea and introduced by John Holland in 1975.

(iv) The application of this technique to the prediction of the ultimate strengths of the WSLC columns such that $0.70 < R_{DL} < 1.60$ yields a=8 and b=12. It is still worth noting that, if the design variables were deemed continuous, the solution would be a=7.70 and b=12.16, causing only a 0.90% decrease in the objective function (3).

Next, the numerical ultimate strengths obtained are compared with their estimates provided (i) by the current DSM L and D strength curves (f_{NL} and f_{ND}) and also (ii) by the DSM approaches specifically developed to deal with L-D interactive failures (NDL, NLD and the generalized MNDL − f_{NDL}, f_{NLD} and f_{MNDL}). The results concerning a representative fraction/sample of the columns identified in Table 1 are presented and discussed − although it is not possible to address all the results obtained (due to space limitations), the sample selected provides enough information

to investigate the how the quality of the DSM ultimate strength predictions vary with the R_{DL} value. The columns considered, which cover the whole R_{DL} range, are WS1-5-9-16-24-27-31-35 (R_{DL}=0.40-0.60-0.80-1.00-1.30-1.60-2.00-2.40). For the sake of clarity, it was decided to (i) begin by addressing the results concerning WSLC columns (Figs. 6-7) and (ii) compare afterwards results concerning WS and plain lipped channel columns with very similar R_{DL} values, *i.e.*, virtually identical levels of L-D interaction (Figs. 9-10). Once again, each of the above 8 columns was analyzed with 9 distinct yield stresses, covering a quite wide critical (D or L) slenderness range.

Figs. 6(a$_1$)-(b$_4$) and 7(a$_1$)-(b$_4$) plot the f_U/f_y values against λ_L and λ_D for the 8 WSLC column sets identified in the previous paragraph. The numerical f_U/f_y values concerning each R_{DL} value are compared with their DSM predictions: (i) f_{NL} or f_{ND}, (ii) f_{NDL} and (iii) f_{MNDL} – the latter adopting the L_{crD}/L_{crL} limits determined earlier (a=8 and b=12), on the basis of the columns with 0.70<R_{DL}<1.60[4]. On the basis of these comparisons, it is possible to extract the following conclusions:

(i)   All the numerical f_U/f_y values are well aligned along "Winter-type" curves.

(ii)   Generally speaking, the observations made by Martins *et al.* (2014a), in the context of plain lipped channel columns, remain qualitatively valid.

(iii)   As it would be logical to expect, for the R_{DL}=0.40 and R_{DL}=0.60 columns the f_{ND} values provide safe and fairly accurate ultimate strength estimates for the whole slenderness range, which means that no perceptible ultimate strength erosion due to L-D interaction occurs. These columns exhibit typical distortional collapse modes and only in quite slender columns minor local deformations were detected (they stem from a "secondary local bifurcation", due to the high yield stress). Fig. 8(a$_1$) concerns a column under these circumstances, more specifically the column with R_{DL}=0.50 and λ_{cr}=3.25, and shows its collapse mode. Fig. 8(a$_2$), providing a close-up of the top flange deformed configuration (amplified 2.5 times), unveils the presence of small (but clearly perceptible) local deformations. Finally, note that $f_{ND} \equiv f_{MNDL}$ for all the R_{DL}=0.40 and R_{DL}=0.60 columns.

(iv)   On the other hand, and also logically, the f_{NL} values provide fairly accurate ultimate strength estimates for the stocky columns with R_{DL}>1.00, since these columns exhibit typical local collapses. For instance, Fig. 8(b$_1$) shows the local collapse mode of the column with R_{DL}=2.40 and λ_{cr}=1.25 (amplified 10 times) – the normal stress redistribution, providing the root of the well-known "effective width concept" originally proposed by von Kármán (von Kármán *et al.* 1932), is clearly illustrated in this figure. As for the "non-stocky" R_{DL}>1.00 columns (R_{DL}=1.30, R_{DL}=1.60, R_{DL}=2.00, R_{DL}=2.40 – Figs. 7(a$_1$)-(a$_4$)), practically all their failure loads are well overestimated by the current DSM L and D design curves, thus providing clear

---

[4]   Since each plot in Figs. 6 and 7 concerns a single column geometry (with several yield stresses), it is possible to present the corresponding MNDL curve, which is associated with the particular L_{crD}/L_{crL} ratio exhibited by that column.
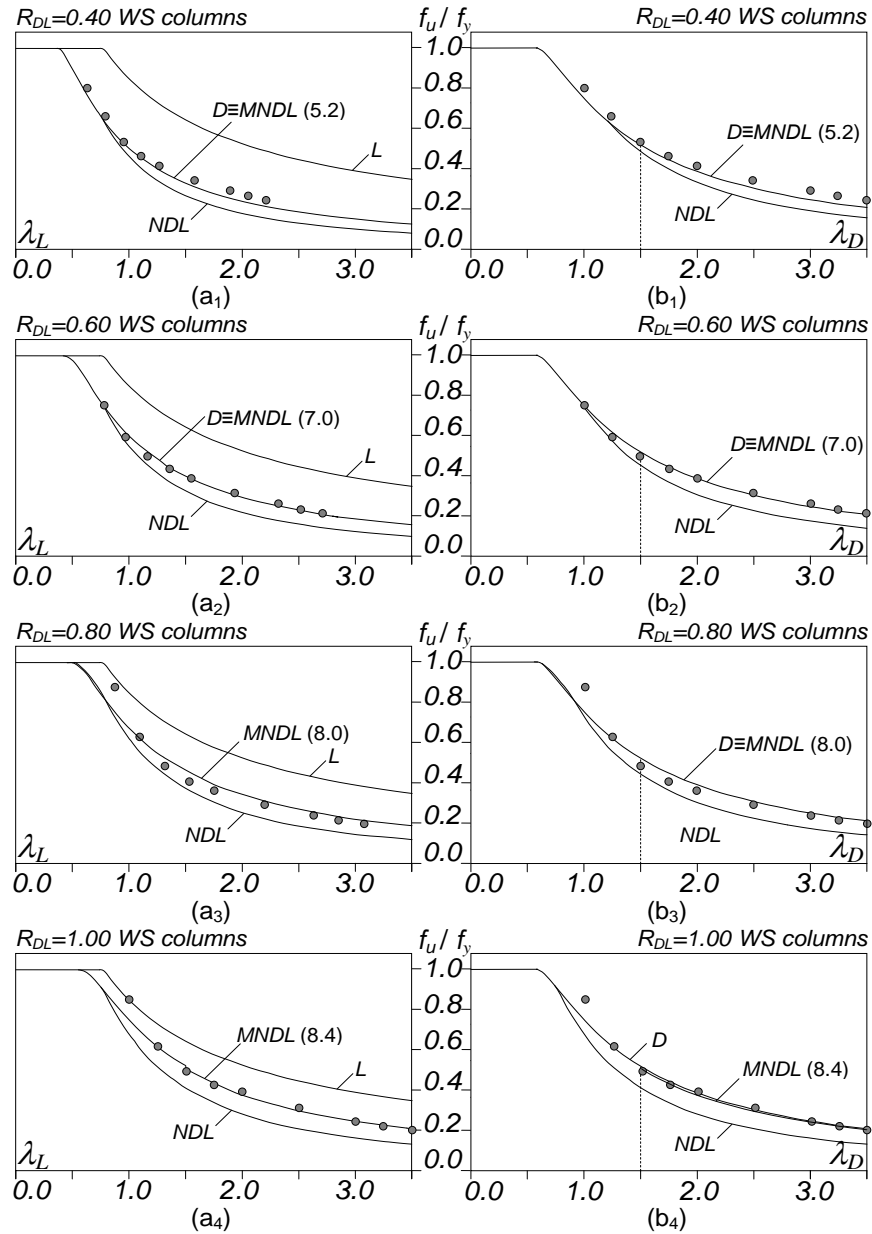
Fig. 6. Variation of f_u/f_y and corresponding DSM predictions with (a) λ_l or (b) λ_d for (1)-(4) R_{DL}=0.40-0.60-0.80-1.00 web-stiffened fixed-ended columns
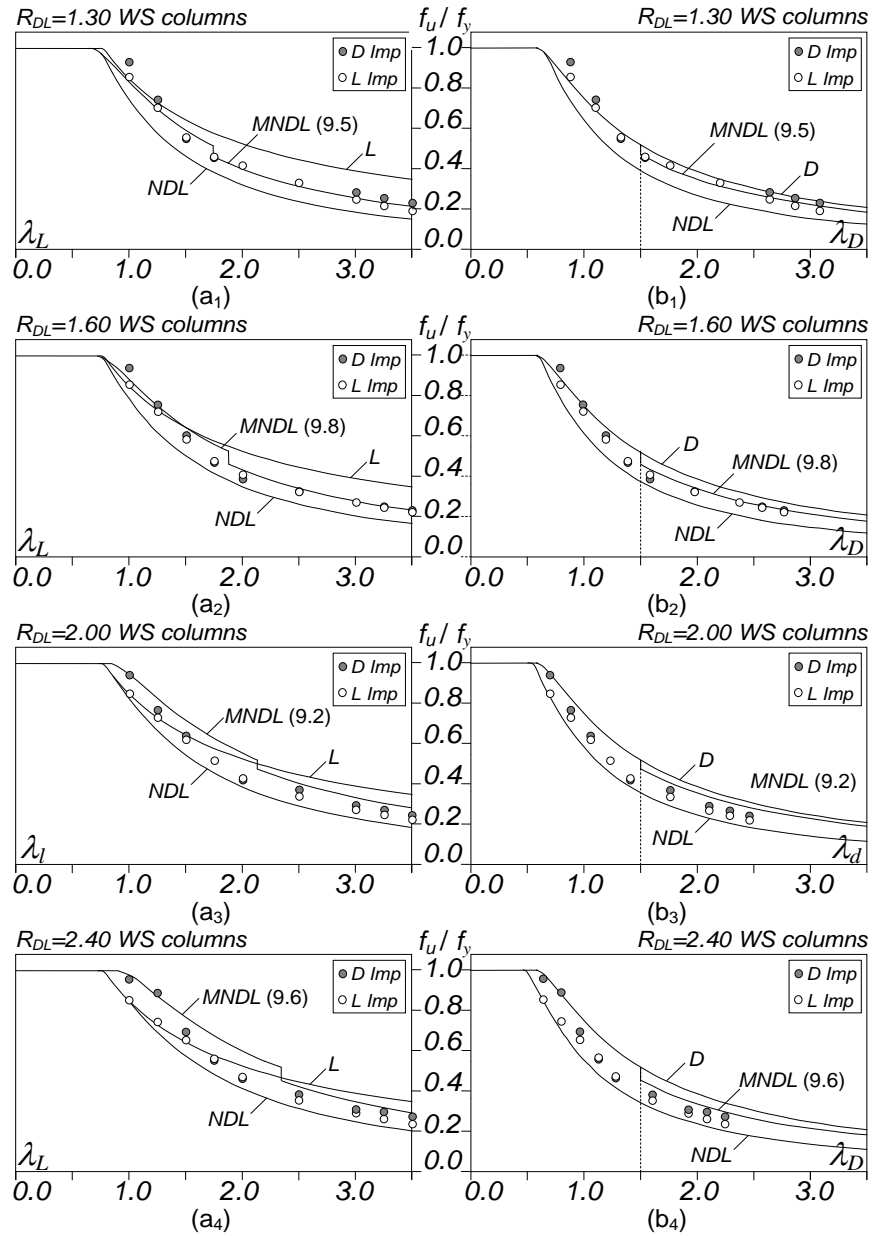
184

Fig. 7. Variation of f_u/f_y and corresponding DSM predictions with (a) λ_l or (b) λ_d for (1)-(4) R_{DL}=1.30-1.60-2.00-2.40 web-stiffened fixed-ended columns

evidence of the occurrence of significant L-D interaction (due to a "secondary distortional bifurcation"). Fig. 8(b$_2$) depicts the L-D interactive collapse mode of the column with R_{DL}=2.40 and λ_{cr}=3.5 (amplified 2 times). Naturally, the λ_{cr} values for which L-D interaction effects becomes less relevant increase with R_{DL}. Moreover, generally speaking, the R_{DL}>1.00 column ultimate strengths tend to be less overestimated by the f_{NL} values as R_{DL} increases (switch from "true L-D interaction" to "secondary distortional bifurcation") and λ_L decreases, since the L-D interaction effects become less relevant – the number of accurate estimates, indicating local failures, grows (slowly) with R_{DL} (see Figs. 7(a$_1$)-(a$_4$)).

(v) As a consequence of what was said in the previous item, the overwhelming majority of the R_{DL}=0.80, R_{DL}=1.00, R_{DL}=1.30 and R_{DL}=1.60 column ultimate strengths are not adequately predicted by the current DSM local or distortional strength curves – only the MNDL approach provides high-quality predictions.

(vi) Naturally, in the R_{DL}=1.00 columns L-D interaction occurs in the whole slenderness range, as clearly shown in Figs. 6(a$_4$)-(b$_4$) – visible difference between the numerical ultimate loads and their f_{ND} estimates. The MNDL approach merits are also evidenced in these figures.

Figs. 9(a$_1$)-(b$_4$) and 10(a$_1$)-(b$_4$) provide the variations of f_U/f_y with λ_L or λ_D for the 8 sets of web-stiffened and plain lipped channel columns – these figures only differ from Figs. 6(a$_1$)-(b$_1$) and Figs. 7(a$_1$)-(b$_1$) in the fact that they include the plain lipped channel results, previously reported by Martins *et al.* (2014a). The aim is to compare the quality of the DSM predictions concerning the two sets of column failure loads, which are associated with similar levels of L-D interaction – note that, in order to improve the readability of these figures, the MNDL design curves are not shown (the assessment of the quality of the f_{MNDL} estimates has just been made). The comparative analysis of all these numerical ultimate strengths prompts the following remarks:

(i) First of all, recall that all the R_{DL}>1.00 columns were analyzed with both L (critical-mode) and D initial imperfections. Although the former invariable led to lower failure loads, most of the differences were quite small (all the exceptions concern stocky columns, for which plasticity precedes distortional buckling).
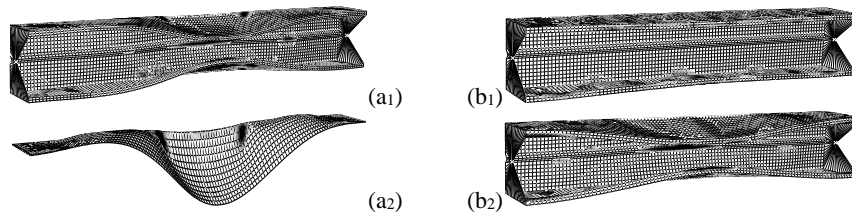

(a$_1$)   (b$_1$)

(a$_2$)   (b$_2$)

Fig. 8. Failure modes and plastic strains of the (a$_1$)-(a$_2$) WS3 column with λ_{cr}=3.5+D (including a top flange close-up), and (b) WS35 columns with (b$_1$) λ_{cr}=1.25+L and (b$_2$) λ_{cr}=3.5+L

(ii) Qualitatively speaking, the results concerning both sets of columns are very similar. Indeed, for identical R_{DL} and slenderness values, the web-stiffened and plain lipped channel column f_U/f_y values are nearly coincident, even if the former are generally a bit higher. It is worth noting that the failure loads of the two sets of columns were obtained considering the most detrimental distortional initial imperfections, which involve inward (outward) flange-lip motions in the web-stiffened (plain) lipped channel columns.

(iii) In view of what was mentioned in the previous item, it seems logical to expect that it may possible to handle jointly the design of web-stiffened and plain lipped channel columns exhibiting L-D interactive failures[5].

Assessment of the Numerical Ultimate Strength Estimates

On the basis of the limited amount of numerical WSLC column failure loads obtained in this work, it is possible to draw some preliminary conclusions concerning the quality of their DSM-based predictions. Figs. 11(a)-(d) plot, respectively, (i) f_U/f_{ND} against λ_L, (ii) f_U/f_{NL} against λ_D, (iii) f_U/f_{NDL} against λ_D and (iv) f_U/f_{MNDL} against λ_D[6]. It should be noted that Figs. 11(a)-(b) include only results concerning columns with $R_{DL} \leq 1.0$ and $R_{DL} > 1.0$, respectively, while Figs. 11(c)-(d) include all the columns analyzed. Moreover, it should be mentioned that f_U is taken as (i) $f_{U,D}$, for $R_{DL} \leq 1.10$, and (ii) the lowest of $f_{U,D}$ and $f_{U,L}$, for $R_{DL} > 1.10$, where $f_{U,D}$ and $f_{U,L}$ are the ultimate strengths determined for columns containing "pure" distortional and "pure" local initial geometrical imperfections. The observation of these figures prompts the following comments:

(i) As mentioned already by several authors, the current DSM design curves (f_{NL} and f_{ND} values) are unable to predict adequately the ultimate strength erosion caused by L-D interaction. The local design curve, whose estimates have very poor indicators (mean and standard deviation equal to 0.79 and 0.14, with a minimum of 0.53) − the only accurate f_{NL} estimates correspond to the stocky columns with high R_{DL} values − *e.g.*, see the columns with $R_{DL}=2.00$ and $R_{DL}=2.40$ in Figs. 11(a$_3$)-(a$_4$)), which fail in pure local modes and, therefore, are not affected by L-D interaction. On the other hand, the f_{ND} predictions exhibit much higher quality, as they are clearly more accurate and mostly safe, which is reflected in the corresponding indicators (mean and standard deviation equal to 1.03 and 0.08, with a minimum of 0.88) − note that the unsafe estimates in Fig. 11(a) concern columns affected by "true" L-D interaction (see also Figs. 6(b$_3$)-(b$_4$)).

(ii) The f_{NDL} values provide only safe ultimate strength estimates, since there is only one f_U/f_{NDL} ratio below (but very close) to 1.0 − see Fig. 11(c) (and also Figs. 6 and

---

[5] The authors are currently working on verifying whether this assertion can also be extended to lipped channel columns with intermediate stiffeners in both the web and flanges.

[6] The inclusion of the apparently "illogical" f_U/f_{ND} vs. λ_L and f_U/f_{NL} vs. λ_D plots (instead of the more "logical" f_U/f_{ND} vs. λ_D and f_U/f_{NL} vs. λ_L ones) was done to improve the plot "readability". This is because, in the latter plots, various ratio values are located on the same vertical line and "on top of each other".
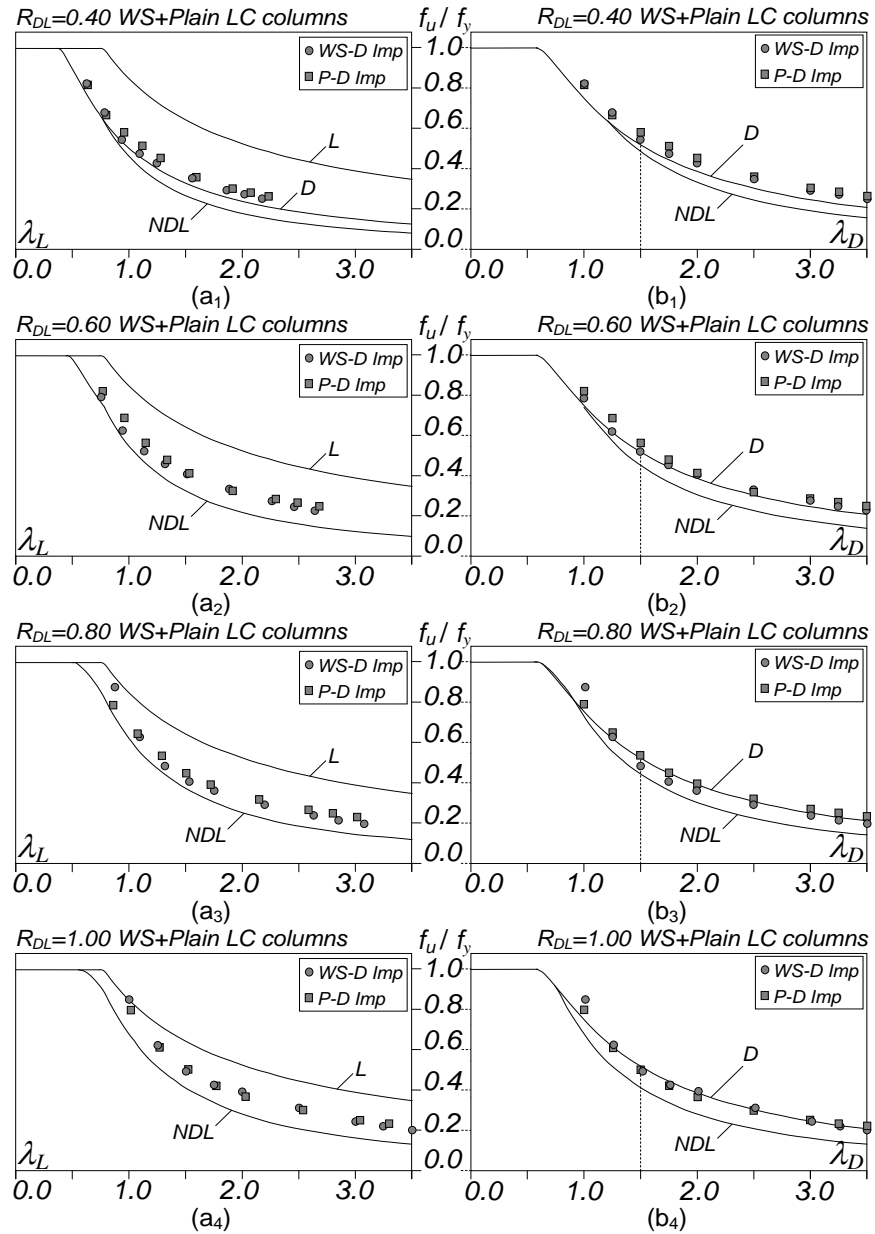
187

Fig. 9. Variation of f_u/f_y and corresponding DSM local and distortional strength predictions with (a) λ_L and (b) λ_D for ($_1$)-($_4$) R_{DL}=0.40-0.60-0.80-1.00 (WS and plain lipped channel columns)
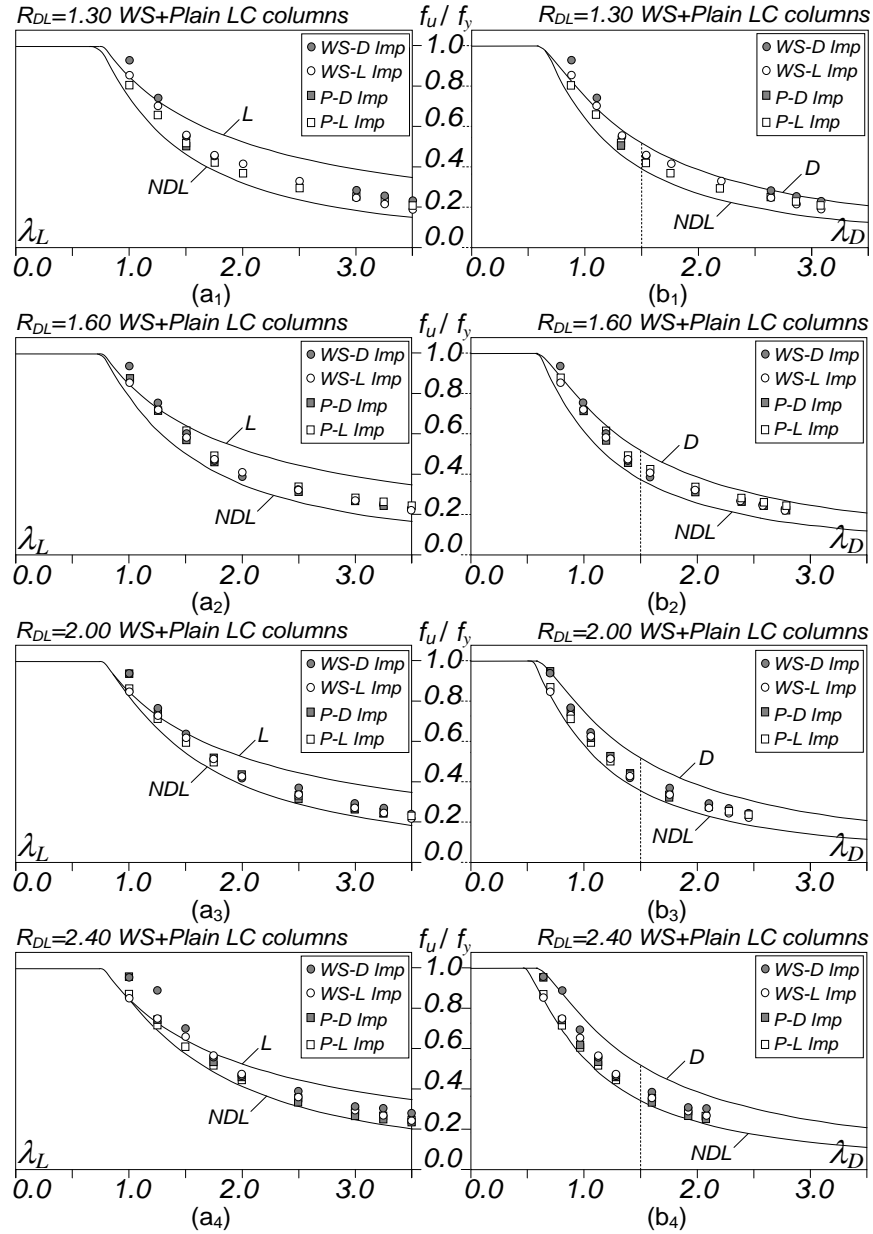
188

Fig. 10. Variation of f_u/f_y and corresponding DSM local and distortional strength predictions with (a) λ_L and (b) λ_D for (1)-(4) R_{DL}=1.30-1.60-2.00-2.40 (WS and plain lipped channel columns)

$7(a_1)$-(b_4)). However, a large fraction of the numerical failure loads are excessively underestimated, particularly in the high slenderness range.

(iii) The f_{MNDL} values provide clearly the best failure load estimates, as can be readily attested by looking at Fig. 11(d) and the corresponding f_U/f_{MNDL} indicators: (iii_1) mean value equal to 1.00, (iii_2) standard derivation equal to 0.07, (iii_3) minimum value equal to 0.84 and (iii_4) maximum value equal to 1.18.
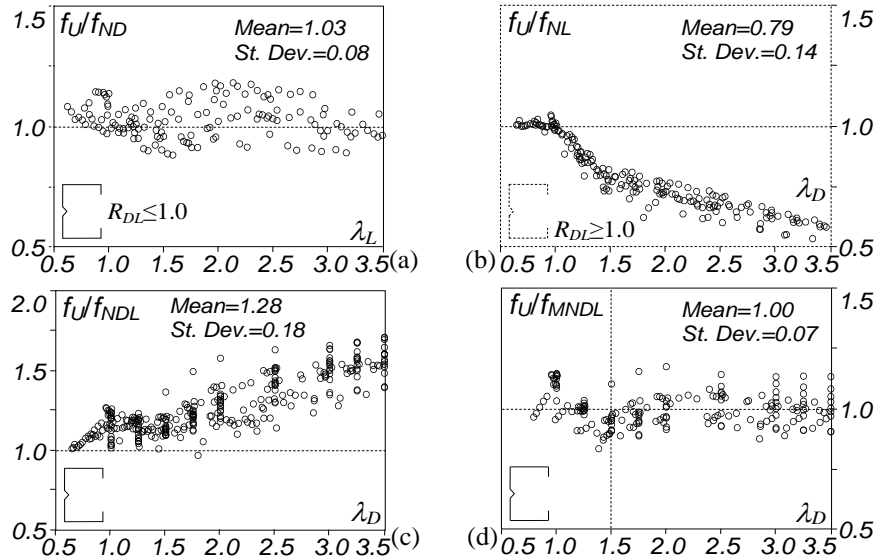

Fig. 11. Plots of (a) f_U/f_{ND} against λ_L, (b) f_U/f_{NL} (c) f_U/f_{NDL} and (d) f_U/f_{MNDL} against λ_D, concerning all the numerical data obtained for web-stiffened lipped channels columns

Conclusion

A numerical investigation on the influence of L-D interaction effects on the post-buckling behavior, ultimate strength and DSM design of cold-formed steel fixed-ended WSLC columns, exhibiting flange-triggered critical local buckling, was reported. All the columns analyzed had geometries (cross-section dimensions and lengths) and yield stresses selected to ensure a wide variety of ratios between the (i) distortional and local critical buckling stresses (R_{DL}), and (ii) yield and non-critical (local or distortional) buckling stresses. ABAQUS geometrically and/or materially non-linear shell finite element analyses were employed to assess the structural response of columns (i) containing critical-mode initial imperfections with small amplitudes (10% of the wall thickness t) and (ii) exhibiting a linear-elastic-perfectly-plastic constitutive law.

After addressing the selection procedure aimed at identifying fixed-ended WSLC columns with different ratios between the distortional and local critical buckling loads (as

well as the output of this procedure), the paper presented a numerical investigation on the elastic and elastic-plastic post-buckling behavior of a selected column with virtually coincident local and distortional critical buckling loads (highest interaction level), with the purpose of acquiring in-depth knowledge about the mechanics underlying the local-distortional interaction phenomenon, when local buckling is triggered by the flanges. Next, an extensive parametric study was performed to gather ultimate strength data concerning fixed-ended WSLC columns (i) containing initial geometrical imperfections exhibiting (i) the most detrimental shape and small amplitudes, (ii) experiencing various L-D interaction "levels" and (iii) having several yield stresses, chosen to cover a wide slenderness range. On the basis of the above numerical ultimate strength data bank, it was possible to assess the quality of their estimates provided by (i) the current DSM local and distortional design curves and (ii) expressions developed specifically to account for the ultimate strength erosion due to L-D interaction effects, namely (i) the NDL and NLD approaches proposed by Schafer (2002), and (ii) a adapted (slightly modified) version of the MNDL approach originally developed by Silvestre *et al.* (2012), which has been shown to provide very efficient estimates for "plain cross-section" columns (Dinis & Camotim 2014, Martins *et al.* 2014a). This quality assessment procedure made it possible to conclude that the findings reported earlier for the "plain cross-section" columns can be extended to WSLC columns exhibiting flange-triggered local buckling.

Finally, one last word to mention that (i) an investigation similar to the one reported in this paper and involving lipped channel columns with intermediate stiffeners in both the web and flanges is currently under away, and (ii) an experimental test program involving web-stiffened lipped channel columns with carefully selected geometries, ensuring flange-triggered local buckling and very clear L-D interaction, is planned for the near future.

Acknowledgements

References

Bebiano R, Pina P, Silvestre N, Camotim D (2008). *GBTUL 1.0β – Buckling and Vibration Analysis of Thin-Walled Members*, DECivil/IST, Technical University of Lisbon.

Dinis PB, Camotim D (2014). Cold-formed steel columns undergoing local-distortional coupling: behaviour and direct strength prediction against interactive failure, *Computers & Structure*, accepted for publication.

Dinis PB, Camotim D, Silvestre N (2007). FEM-based analysis of the local-plate/distortional mode interaction in cold-formed steel lipped channel columns, *Computers & Structures*, **85**(19-20), 1461-1474.

Dinis PB, Camotim D, Fena R (2011). Local/distortional mode interaction in hat-section columns: post-buckling behaviour, strength and DSM design, *Proceedings of 6th European Conference*

on Steel and Composite Structures, (EUROSTEEL 2011 – Budapest, 31/8-2/9), 69-74.

Dinis PB, Camotim D, Fena R (2012). Post-buckling, strength and design of cold-formed steel lipped channel, zed-section and hat-section columns affected by local-distortional interaction, *USB Proceedings of SSRC Annual Stability Conference* (Grapevine – 18-21/4).

Dinis PB, Young B, Camotim D (2014a). Local-distortional interaction in cold-formed steel rack-section columns, *Thin-Walled Structures*, **81**(August), 185-194.

Dinis PB, Young B, Camotim D (2014b). Strength, interactive failure and design of web-stiffened lipped channel columns exhibiting distortional buckling, *Thin-Walled Structures*, **81**(August), 195-209.

Hancock GJ, Kwon YB, Bernard ES (1994). Strength design curves for thin-walled sections undergoing distortional buckling, *Journal of Constructional Steel Research*, **31**(2-3), 169-186.

Kwon YB, Hancock GJ (1992). Tests of cold-formed channels with local and distortional buckling, *Journal of Structural Engineering* (ASCE), **118**(7), 1786-1803.

Kwon YB, Kim BS, Hancock GJ (2009). Compression tests of high strength cold-formed steel channel with buckling interaction, *Journal of Constructional Steel Research*, **65**(2), 278-289.

Martins AD, Dinis PB, Camotim D, Providência P (2014a). On the relevance of local-distortional interaction effects in the behaviour and design of cold-formed steel columns, *USB Proceedings of SSRC Annual Stability Conference* (Toronto, 25-28/3).

Martins AD, Dinis PB, Camotim D, Providência P (2014b). Local-distortional interaction in web-stiffened LC columns: Post-buckling behaviour, strength and DSM design, *Proceedings of 7th European Conference on Steel and Composite Structures* (EUROSTEEL 2014, Naples, 10-12/9).

Schafer BW (2002). Local, distortional and Euler buckling in thin-walled columns, *Journal of Structural Engineering* (ASCE), **128**(3), 289-299.

Schafer BW (2008). Review: the direct strength method of cold-formed steel member design, *Journal of Constructional Steel Research*, **64**(7-8), 766-778.

Schafer BW, Peköz T (1998). Direct strength predition of cold-formed steel members using numerical elastic buckling solutions, *Thin-Walled Structures – Research and Development* (ICTWS'98 – Singapore, 2-4/12), N. Shanmugam, J.Y.R. Liew, V. Thevendran (eds.), Elsevier, 137-144.

Silvestre N, Camotim D, Dinis PB (2012). Post-buckling behaviour and direct strength design of lipped channel columns experiencing local/distortional interaction, *Journal of Constructional Steel Research*, **73**(June), 12-30.

Simulia Inc. (2008), *ABAQUS Standard* (version 6.7-5).

von Kármán T, Sechler EE, Donnell LH (1932). The strength of thin plates in compression, *Transactions of the American Society of Mechanical Engineers* (ASME), **54**, 53-57.

Yang D, Hancock GJ (2004). Compression tests of high strength steel channel columns with interaction between local and distortional buckling, *Journal of Structural Engineering* (ASCE), **130**(12), 1954-1963.

Yap DCY, Hancock GJ (2009). Post-buckling in the distortional mode and buckling mode interaction of cold-formed thin-walled sections with edge stiffeners, *Proceedings of 18th International Specialty Conference on Cold-Formed Steel Structures* (CCFSS 2006 – Orlando, 26-27/10), 71-88.

Yap DCY, Hancock GJ (2011). Experimental study of high strength cold-formed stiffened-web C-sections in compression, *Journal of Structural Engineering* (ASCE), vol. **137**(2), 162-172.

Young B, Silvestre N, Camotim D (2013). Cold-formed steel lipped channel columns influenced by local-distortional interaction: strength and DSM design, *Journal of Structural Engineering* (ASCE), **139**(6), 1059-1074.